Climate Dynamics (2026) 64:43
https://doi.org/10.1007/s00382-025-08016-9

ORIGINAL ARTICLE

Characterizing dry and humid heatwaves in Southern South America: regional trends and large-scale climate drivers

Agustina Lopez-Ramirez[1,2] · Mariana Barrucand[1,2] · Soledad Collazo[1,3,4]

Received: 19 August 2025 / Accepted: 7 December 2025

Abstract

This study characterizes the spatiotemporal variability of heatwaves occurring under dry and humid conditions during the warm season (October–March) in southern South America (SSA) between 1979 and 2018. Using daily maximum temperature and precipitation data from 132 meteorological stations, we identified compound extremes based on the co-occurrence (simultaneous or sequential) of heatwaves with anomalously dry or wet conditions, defined by the Standardized Precipitation Index. Four types of compound events were analyzed: simultaneous and sequential dry heatwaves (SIDH, SEDH), and simultaneous and sequential humid heatwaves (SIHH, SEHH). SIDH and SEDH were the most common compound events, particularly in northeastern and central Argentina, while humid events (SIHH and SEHH) were generally less frequent, especially SIHH. Changes in frequency, duration, intensity, and spatial extent of compound heatwaves were examined by comparing two subperiods (1979–1998 and 1999–2018). Our findings show an increase in the frequency and spatial extension of dry events (SIDH and SEDH) and SEHH in recent decades. We also investigated the influence of large-scale climate drivers—El Niño–Southern Oscillation, Pacific Decadal Oscillation (PDO), Indian Ocean Dipole (IOD), and Southern Annular Mode (SAM)—and their combined phases on compound heatwave occurrence. In particular, the concurrent occurrence of La Niña, negative PDO, negative IOD, and positive SAM phases was associated with an increased occurrence of dry compound heatwaves and a reduction in humid ones. These findings highlight the importance of understanding compound heatwaves, especially in regions like SSA where land–atmosphere feedbacks and climate variability strongly influence extremes.

Keywords Compound event · Climate extremes · Maximum temperature · Precipitation · ENSO · PDO

1 Introduction

The Intergovernmental Panel on Climate Change defines compound events as the occurrence of two or more extremes, either simultaneously or in sequence; when the combination of different extremes leads to amplified impacts or when events that are not extreme on their own result in an extreme outcome when they occur together, creating emergent risks (Seneviratne et al. 2012). Such events often exceed the capacity of ecosystems and societies to respond, causing significant disruptions to health, socioeconomic systems, agriculture, and natural environments (Jiang and Huang 2000; Flannigan et al. 2009; Allen et al. 2010; Ben-Ari et al. 2018; Wang et al. 2019; Raymond et al. 2020).

Hot and dry conditions are among the most extensively studied hydrometeorological compound events (Ridder et al. 2020; Ionita et al. 2021; Bevacqua et al. 2022; Wu and Jiang 2022; De Luca and Donat 2023). A critical element

✉ Agustina Lopez-Ramirez
alopez@at.fcen.uba.ar

1 Facultad de Ciencias Exactas y Naturales, Departamento de Ciencias de La Atmósfera y los Océanos (DCAO-FCEN-UBA), Universidad de Buenos Aires, Buenos Aires, Argentina

2 Consejo Nacional de Investigaciones Científicas y Técnicas (CONICET), Buenos Aires, Argentina

3 Departamento de Física de La Tierra y Astrofísica, Facultad de Ciencias Físicas, Universidad Complutense de Madrid, Madrid, Spain

4 Instituto de Geociencias (IGEO), Consejo Superior de Investigaciones Científicas-Universidad Complutense de Madrid (CSIC-UCM), Madrid, Spain

Published online: 06 January 2026

in the development of these events is the feedback between air temperature and soil moisture. Deficits in moisture limit evapotranspiration and latent heat flux, resulting in increased warming of the air through sensible heat fluxes (Seneviratne et al. 2010; Mueller and Seneviratne 2012). This additional warming raises the evaporative demand, which further exacerbates moisture deficits and drives temperatures even higher.

In South America, extended precipitation deficits are significant predictors of hot summer days in northern-central Argentina (Collazo et al. 2019). The probability of experiencing a higher-than-average number of warm days can increase up to 70% following a precipitation deficit, while it declines to 30–40% after wet conditions. This difference is linked to enhanced soil-atmosphere interactions during dry spells in southeastern South America (Spennemann et al. 2018). Furthermore, recent research indicates that the coupling between soil moisture and the atmosphere, along with drier soil conditions, plays a key role in the rise of temperature extremes in the region (Coronato et al. 2020). The interaction between soil and atmosphere, as well as variability in soil moisture, are crucial for the onset and persistence of warm days.

In contrast to the extensive research on hot and dry events, hot and humid conditions represent another type of hydrometeorological compound event that has received less attention. Most studies focus on specific case analyses, and there is a lack of theoretical frameworks addressing the mechanisms involved (Zhang et al. 2021). Nevertheless, scientific literature indicates that the stability and persistence of large-scale atmospheric circulation patterns are crucial for the occurrence of these events (Guo et al. 2023). In southern South America (SSA), during the warm season, a dipole pattern characterized by negative geopotential height anomalies at 500 hPa over the Pacific Ocean and positive anomalies over the Atlantic Ocean promotes the influx of warm, humid air from lower latitudes into northeastern Argentina and southeastern South America. This influx enhances atmospheric instability, leading to an increased likelihood of hot and humid events in these regions (Olmo et al. 2020).

Other studies have focused on the variability of hot and humid events and the observed changes in recent years. For instance, Hao et al. (2013) highlighted a rising trend in the concurrent occurrence of hot and humid extremes, especially at high latitudes and in tropical regions, using data from meteorological stations and simulations from the Coupled Model Intercomparison Project Phase 5. In South America, Tencer et al. (2016) found that during the warm season (October to March), intense precipitation in eastern Argentina often occurs simultaneously with or shortly after extremely hot days, while such events rarely precede them. In contrast, cold days tend to follow intense precipitation events more frequently. Subsequently, Olmo et al. (2020) reported that extreme temperatures (warm nights and cold days) significantly increase the likelihood of heavy rainfall, particularly in southern Chile and southeastern South America.

Large-scale climate drivers, such as El Niño–Southern Oscillation (ENSO), influence compound temperature and precipitation extremes across multiple regions and seasons (Mukherjee et al. 2020; Zhang et al. 2021; Hao et al. 2022). Several studies have identified specific atmospheric circulation patterns as key mechanisms linking these large-scale drivers to compound extremes. For instance, the relationship between ENSO and extratropical climate anomalies is mediated by Rossby wave trains, particularly the Pacific–South America patterns, which enhance the subtropical jet stream (Cai et al. 2020; Reobita et al. 2021).

The ENSO teleconnection pattern often interacts with other large-scale drivers rather than acting independently, and their impacts can be modulated or amplified. For example, Andreoli and Kayano (2005) and Gamelin et al. (2020) found that the phase of PDO influences the strength and spatial extent of ENSO-related teleconnections, with more coherent and intense effects during the PDO's cold phase. Andrian et al. (2024) showed that positive IOD events can reinforce El Niño-induced circulation anomalies, while negative IOD/La Niña combinations produce weaker effects. Another example is that El Niño events are typically associated with the negative phase of SAM, whereas La Niña events are more often linked to its positive phase (Carvalho et al. 2005; Fogt et al. 2011). One proposed mechanism is that positive sea surface temperature anomalies associated with El Niño raise global mean temperatures and contribute to lower pressure over midlatitudes (Wang and Cai 2013). Despite these insights, the joint influence of multiple climate modes on compound events has received limited attention.

Building on these discussions, this study aims to characterize the spatiotemporal variability of heatwaves occurring under both dry and humid conditions during the warm season (October–March) in SSA over the 1979–2018 period. Using daily data from 132 meteorological stations, we assess regional differences and trends in their frequency, duration, intensity, and spatial extent. Additionally, we investigate how individual and combined phases of four climate drivers (ENSO, PDO, IOD, and SAM) modulate the occurrence and spatial extension of these events.

2 Data and methods

2.1 Data and study region

This research uses daily maximum temperature and precipitation records from 132 meteorological stations situated in SSA (Fig. 1) over the warm season (October to March) from 1979 to 2018. The stations were classified according to the heatwave regionalization established by Suli et al. (2023). This classification uses Ward hierarchical clustering method to determine 5 different regions: northern of SSA (1. NS), central-eastern of SSA (2. CES), central Argentina and northern Argentinian Patagonia (3. CA), central Chile (4. CCH), Argentinian Patagonia and southern Chile, southern SSA (5. SS). We additionally considered the four northern stations in Chile as a new region (6. NCH). A thorough quality control process was implemented for all datasets to detect potential errors, outliers, or inconsistencies.

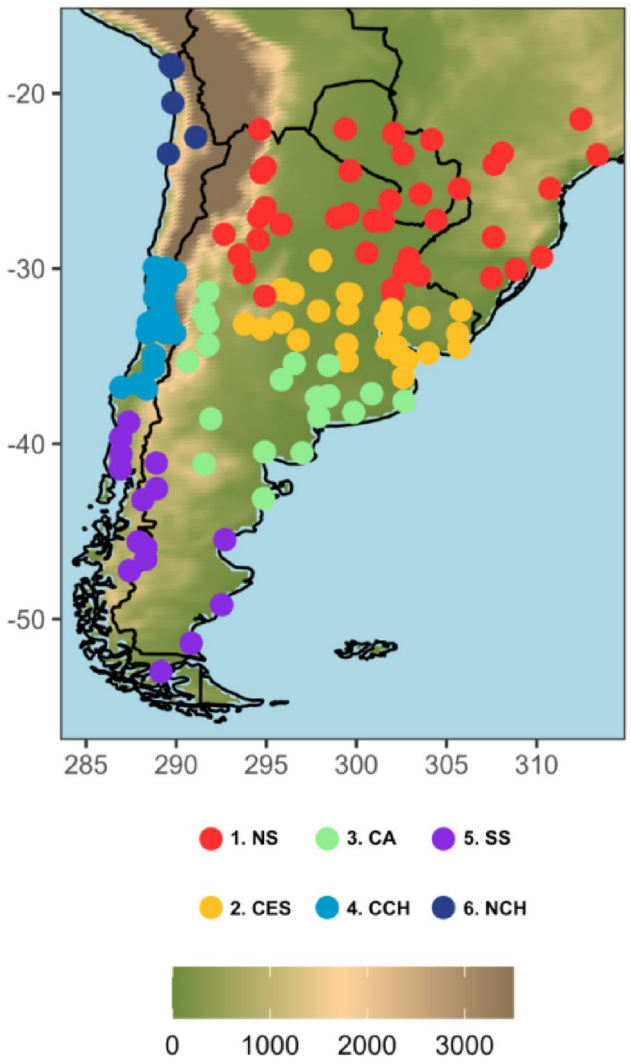

Fig. 1 Meteorological stations used in this study, categorized by region (1.NS: northern of SSA, 2.CES: central-eastern of SSA, 3.CA: central Argentina and northern Argentinian Patagonia, 4.CCH: central Chile, 5.SS: southern SSA, 6.NCH: northern Chile). The shaded colors represent the elevation of SSA based on ERA5 reanalysis, expressed in meters [m]

2.2 Definition of compound heatwave

Compound events were characterized by the simultaneous or sequential occurrence of heatwaves with deficits or excesses in precipitation. Heatwaves were identified as periods when the maximum temperature exceeded the 90th percentile (calculated based on the 1981–2010 period with a 15-day moving window) for at least three consecutive days. Precipitation deficits and excesses were assessed using the Standardized Precipitation Index (SPI). The SPI is a widely used metric in climatological studies to evaluate and quantify drought or excessive moisture conditions within a specific geographic area and timeframe. It is calculated over various time scales, including 1, 3, 6, and 12 months, with values grouped into categories to define drought and excess moisture (McKee et al. 1993). An SPI value of less than -1 indicates severe drought conditions, while a value greater than 1 indicates severe wet conditions. In this study we used the SPI for one-month (SPI1) and three-month (SPI3) durations. The SPI1 is highly sensitive to recent precipitation anomalies and is useful for detecting short-term fluctuations, while the SPI3 better captures meteorological droughts and seasonal-scale precipitation variability.

In this context, we identified simultaneous dry heatwaves (SIDH), which coincide with drought conditions (SPI1 <-1 and SPI3 <-1); sequential dry heatwaves (SEDH), characterized by droughts followed by heatwaves (SPI1 >-1 and SPI3 <-1); simultaneous humid heatwaves (SIHH), defined by concurrent heatwaves and excessive moisture (SPI1 >1 and SPI3 >1); and sequential humid heatwaves (SEHH), where heatwaves are followed by moisture excesses (SPI1 month $i<1$ and SPI3 month $i+2>1$). We considered the SPI1 and SPI3 of the month where the heatwave occurred for all event types, with the exception of SEHH. For this last event, we used the SPI3 value two months after the heatwave occurrence in order to capture the moisture excesses after the heatwave. These classifications aim to capture different hydroclimatic contexts. In the case of simultaneous events, both SPI1 and SPI3 indicate the presence of persistent dry or humid conditions that are already well established at the time of the heatwave. In contrast, sequential events reflect a shift in moisture conditions, where the soil moisture changes over time: either a heatwave emerges after a prolonged drought (SEDH) or excess moisture develops after a heatwave (SEHH). By using both short-term (SPI1) and medium-term (SPI3) indices, we obtain a more comprehensive view of the surface conditions, allowing us to better

represent the potential influence of soil moisture and precipitation anomalies on compound events. These four compound event definitions can be found in Table 1. In addition to these compound events, individual heatwaves were also analysed, defined as heatwave occurrences regardless of precipitation conditions.

2.3 Spatiotemporal variability

To explore the spatiotemporal variability of the events and changes in their occurrence frequency, the study period was divided into two subperiods: an earlier period (1979–1998) and a more recent one (1999–2018). We assessed changes by comparing the total event frequencies and the number of compound heatwave days (CoHWds) across both periods. We define CoHWds as the number of days involved in a heatwave with dry or humid conditions, either simultaneous or sequential. Specifically, we identified meteorological stations where the frequency and CoHWds in the more recent phase were either less than half, between half and double, or greater than double compared to the earlier period.

We also examined the empirical cumulative distribution functions (ECDF) of the spatial extent of the events. The spatial extent was defined as the proportion of stations experiencing at least one event during the warm season relative to the total number of stations across the entire study domain. The ECDF visually represents how values are distributed. In this analysis, we used the ECDF to detect differences in spatial extent between the two subperiods. Statistical significance was determined using the Kolmogorov–Smirnov test (Smirnov 1939).

Subsequently, we investigated the interannual variation in CoHWds, along with the intensity, duration, and spatial extent of compound heatwaves. Time series of CoHWds were calculated as the total count of days involved in compound heatwaves for each summer. Duration was defined as the annual average number of days each event persisted, while intensity was assessed as the difference between the maximum temperature on the heatwave day and the 90th percentile, averaged across all days of the heatwave. As well as the duration, the intensity was also averaged annually.

Table 1 Description of the compound event definition considered in this work. All SPI1 and SPI3 values correspond to the month in which the heatwave occurred for all event types, except for SEHH

Event type	Tmax	SPI 1	SPI 3
Simultaneous dry heatwave (SIDH)	>P90 for at least three consecutive days	<-1	<-1
Sequential dry heatwave (SEDH)		>-1	<-1
Simultaneous humid heatwave (SIHH)		>1	>1
Sequential humid heatwave (SEHH)		<1	>1[1]

[1]Considering the SPI3 value two months after the heatwave occurrence

Lastly, we computed the spatial averages of CoHWds, duration, and intensity, considering all meteorological stations within the study region and for each specific subregion of SSA. Only stations that recorded compound events were included in the spatial averaging.

2.4 Climate drivers

The influence of four climate drivers was analyzed in this study. The ENSO was represented using the Oceanic Niño Index (ONI), which is calculated as the 3-month running mean of sea surface temperature (SST) anomalies in the Niño 3.4 region (120°W–170°W, 5°N–5°S). ONI values of +0.5 or higher indicate El Niño conditions, while values of −0.5 or lower indicate La Niña. The ONI data, available on the Climate Prediction Center's website (http://www.cpc.ncep.noaa.gov/), were analyzed on a trimestral scale.

To capture other large-scale influences, the PDO, IOD, and SAM indices were also analyzed. The PDO index (available on https://psl.noaa.gov/data/climateindices/list/) is derived using principal component analysis of monthly SST anomalies in the North Pacific, from 20°N to the pole. A positive PDO phase occurs when SSTs are anomalously cold in the central North Pacific and warm along the North American coast, while sea-level pressures over the North Pacific are below average. Conversely, a negative PDO phase corresponds to reversed SST and pressure patterns.

The IOD index (available on https://www.cpc.ncep.noaa.gov/products/international/ocean_monitoring/indian/IODDMI/DMI_month.html) reflects the SST anomaly gradient between the western equatorial Indian Ocean (50°E–70°E, 10°S–10°N) and the southeastern equatorial Indian Ocean (90°E–110°E, 10°S–0°N). During a positive IOD phase, warm waters accumulate in the western Indian Ocean, while upwelling of cold deep waters occurs in the eastern Indian Ocean. This pattern reverses during the negative phase.

Finally, the SAM index (available on http://www.nerc-bas.ac.uk/icd/gjma/sam.html) was defined by Marshall (2003) and represents the strength of the mid-to-high latitude meridional pressure gradient over Antarctica and circumpolar zonal winds. A positive SAM phase is associated with a poleward shift and intensification of the westerly winds, while a negative phase reflects a weaker pressure gradient and equatorward shift of the westerlies.

PDO, IOD, and SAM were analyzed on a monthly scale. To assess potential previous influences, the phase of each climate driver was determined based on the month preceding each compound heatwave. For the ONI index, which is on a trimestral scale, we used the trimester centered on the month prior to each compound heatwave. For each climate driver and phase, we calculated the relative frequency of each event type. To assess whether the occurrence of

compound heatwaves is significantly associated with the different phases of each driver, we applied a Fisher's exact test (at the 95% confidence level) to evaluate the dependence between the phase category (e.g., El Niño, Neutral, La Niña) and the presence or absence of each compound event type.

To assess combined influences, 24 Driver Combinations (DCs) were defined based on all possible combinations of ENSO (El Niño, Neutral, La Niña), PDO (positive/negative), IOD (positive/negative), and SAM (positive/negative). Each warm-season month during the study period was assigned to one of these DCs based on the phases of the four drivers. In order to compare these DCs months with compound heatwave occurrences at the same time scale, we identified months with at least one station of the region affected by a compound heatwave. Then, the role of each DC was evaluated by computing the conditional probability of each compound heatwave type across SSA subregions. The conditional probability represents the ratio between the frequency of months with compound heatwaves under a specific DC and the total frequency of months with compound heatwaves throughout the study period. Additionally, the percentage of stations affected by each event was calculated to assess the spatial extent of each DC's influence.

3 Results

3.1 Spatial distribution of compound heatwaves

To characterize compound heatwaves, we calculated their absolute frequencies over the entire study period (Fig. 2). Both SIDH and SEDH share a similar spatial distribution, with the highest frequencies concentrated in central and northeastern Argentina. In Chile, however, fewer events were observed in the central and northern regions, while there was an increase in frequency towards the south, particularly for SEDH. In southern Chile and western Patagonia, up to 10 to 18 events were recorded over the study period.

On the other hand, humid heatwaves were less frequent than dry heatwaves. SIHH events were the least common of all compound heatwaves in SSA, with substantially fewer frequencies than the other types. SEHH were slightly more frequent across the study region, especially in the east. However, both event types had low frequencies in northwestern Argentina and northern Chile. In central-eastern Argentina and Uruguay, stations observed as many as 14 SEHH events throughout the period. Similarly, in central Chile, some locations experienced up to 10 SEHH events. This high frequency was also evident at a station in western Patagonia, where between 12 and 14 SEHH events occurred.

To assess the importance of compound events, we analyzed the frequency of individual heatwaves and the proportion of those that coincided with dry or humid conditions (Figure S1 in Online Resource 1). In several areas, especially over eastern and northeastern Argentina and Uruguay, compound heatwaves represent nearly half of all heatwave occurrences, highlighting their climatic relevance compared to individual heatwaves alone. These results show that heat extremes in the region are strongly influenced by precipitation variability rather than occurring independently from it.

The northern region of Chile stands out as a distinct region in SSA where the occurrence of compound heatwaves was extremely rare. Given the consistently low number of events across all event types, this region was not included in the subsequent regional analyses.

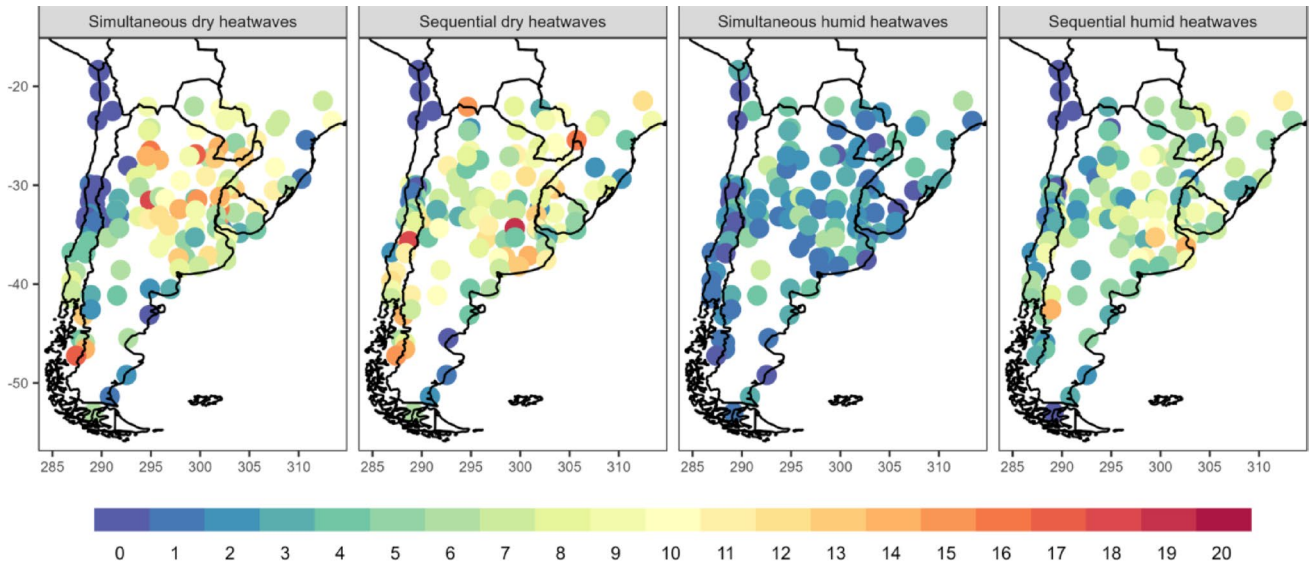

Fig. 2 Absolute frequencies of SIDH, SEDH, SIHH, and SEHH during the period 1979–2018

3.2 Frequency changes between early and recent periods

The study period was divided into two 20-year sub-periods: 1979–1998 and 1999–2018. This division allowed us to explore changes in the frequency of compound heatwaves between the earlier and more recent periods (Fig. 3). Although there was an absence of a unifying increase or decrease in frequency across SSA, some local patterns were observed.

In the case of SIDH, several stations in central and northeastern Argentina, as well as in southern Chile and northern Brazil, showed significant positive differences, with frequencies in the recent period exceeding twice those of the earlier period. In contrast, four stations located in central and northern Argentina exhibited negative differences. In these stations, the frequency in the recent period fell to less than half of what was previously observed.

For SEDH, positive differences were observed in central and northwestern Argentina, central Chile, northern Paraguay, and eastern Brazil. However, certain stations, particularly in western Argentina and eastern Uruguay, experienced a decrease in event frequency, with values falling to less than half of those recorded during the earlier period.

For SIHH, positive differences were observed in northern Argentina, northern Chile, and several stations in Brazil, indicating an increase of up to five additional events in the recent period. In contrast, negative differences were observed in two stations in central and northwestern Argentina. In Patagonia and southern Chile, the differences were nearly zero, reflecting no significant changes in event frequency in this region.

For SEHH, larger differences were found compared to simultaneous events. Positive differences were evident in much of the study area, particularly in southern Chile, eastern Argentina, Uruguay, and Brazil, with some stations experiencing at least five additional events in the recent period. In contrast, negative differences were identified in Paraguay and several adjacent stations in Argentina and Brazil.

In addition to the study of event frequency differences, we also analyzed the differences in the total number of CoHWds between the two periods (Figure S2 in Online Resource 1). Overall, the spatial patterns were largely consistent with those observed for frequency.

3.3 Changes in spatial extent

Building on the previous analysis, we examined the ECDF of the spatial extent of compound heatwaves during the earlier and more recent periods (Fig. 4). These ECDFs allowed us to identify differences in the spatial extent of events between the two time periods.

The ECDFs of SIDH, SIHH, and SEHH from the earlier period show a more rapid growth than those from the recent period. This difference in growth rate indicates a change in the distribution of spatial extent over time. For instance, the ECDF of SIDH reached a 100% probability at 0.26 (26% of the meteorological stations) in the earlier period, while in the recent period, it reached 0.33 (33% of the stations). This suggests that, in the recent period, SIDH exhibited a

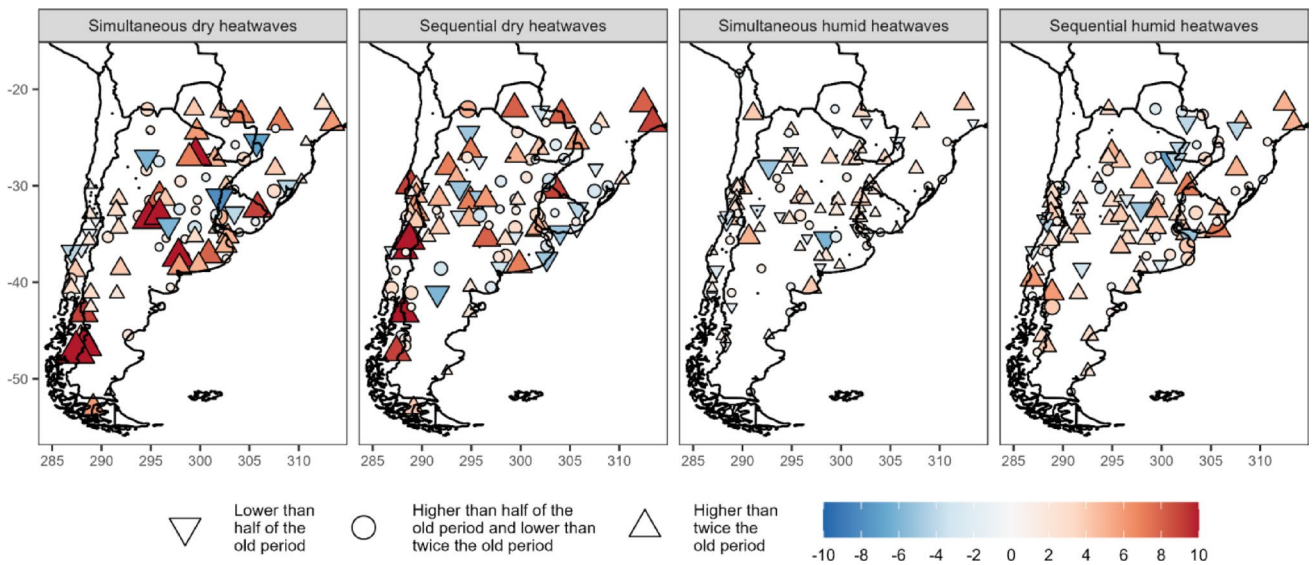

Fig. 3 Difference in frequencies between the periods 1999–2018 and 1979–1998 for SIDH, SEDH, SIHH, and SEHH. Stations where the frequency in the recent period was more than double that of the earlier period are indicated with upward triangles, while those with frequencies less than half are marked with downward triangles. The remaining cases are represented by circles. Marker size and color both reflect the magnitude of the difference in frequencies, with larger and darker symbols indicating larger differences

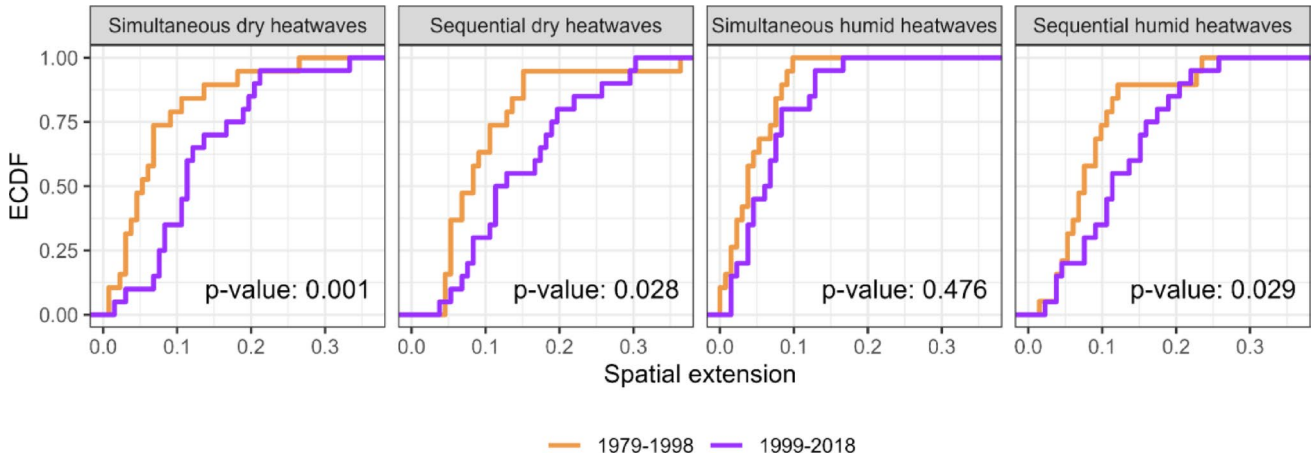

Fig. 4 ECDF of the spatial extent of SIDH, SEDH, SIHH, and SEHH. The *p*-values from the Kolmogorov–Smirnov test between distributions are indicated. Spatial extension expressed as the percentage of stations with at least one event during the warm season

greater spatial extent compared to the earlier period. A similar pattern was observed for humid heatwaves, particularly for SEHH, where this difference is statistically significant.

The ECDF of SEDH also shows a more abrupt growth in the earlier period; nevertheless, unlike the other compound event types, it reaches a 100% probability at higher values of spatial extent than those observed in the recent period (0.36 compared to 0.30, respectively). In this case, most SEDH events from the recent period exhibited a bigger spatial extent compared to those from the earlier period, as indicated by the difference in growth rate of the ECDF. However, a single event with relatively high spatial extent in the earlier period contributes to the higher maximum value.

3.4 Temporal and regional trends

We examined the temporal variability of compound heatwaves through an analysis of interannual changes in the number of CoHWds, duration, intensity, and spatial extent across the study region (Fig. 5). Significant positive trends were observed in the CoHWds of SIDH and SEDH, indicating an increase in the number of days involved in these events over the years. The spatial extent of SIDH also showed a significant increment, suggesting an expansion of these events throughout SSA. In contrast, no significant changes were found in the duration or intensity of dry heatwaves, whether simultaneous or sequential, suggesting that the observed increase in CoHWds of dry events is primarily due to a higher frequency of events rather than longer ones. This is further supported by Fig. 3, which shows that the number of events in the recent period is at least twice as high as in the earlier period for most stations.

For humid heatwaves, significant positive trends were observed in both duration and spatial extent of SIHH. However, no significant changes were detected in their intensity or in the number of CoHWds. In the case of SEHH, both duration and intensity have remained unchanged over time, while the total number of CoHWds and the spatial extent of these compound events have increased.

Similar to some compound heatwaves, positive and significant trends were also found for the number of heatwave days and spatial extent of individual heatwaves (Fig. S3 in Online Resource 1). However, the contribution of compound events to the total number of heatwaves and their variability differs depending on the type of event considered (Figs. 2 and 5).

It is important to highlight that in 1981 and 1989, no SIHH were recorded. This results in a drop to zero in the spatial extent and a break in CoHWds, duration and intensity during those years due to the absence of events. The absence of SIHH is related to specific climatic conditions during those years. In 1989, a strong La Niña event produced warm and dry conditions over most of the study area (Lopez-Ramirez et al. 2024), which explains the high frequency of dry heatwaves and the lack of humid ones. In contrast, summer 1981 was unusually cool, limiting the occurrence of heatwaves (Figure S3 in Online Resource 1) and resulting in very low spatial extent values across all compound categories.

While the global average for the studied domain provides important insights, it is essential to acknowledge that compound heatwaves may exhibit regional behaviors that a global analysis might miss. Therefore, we assessed the trends in time series averaged by region (Fig. 6).

Regarding CoHWds, significant positive trends were observed for SIDH in Regions 2 (CES), 3 (CA), and 5 (SS), whereas SEDH showed increases only in Region 4 (CCH). Among humid events, SEHH exhibited significant positive trends in Regions 3 (CA), while SIHH showed no significant changes across any region.

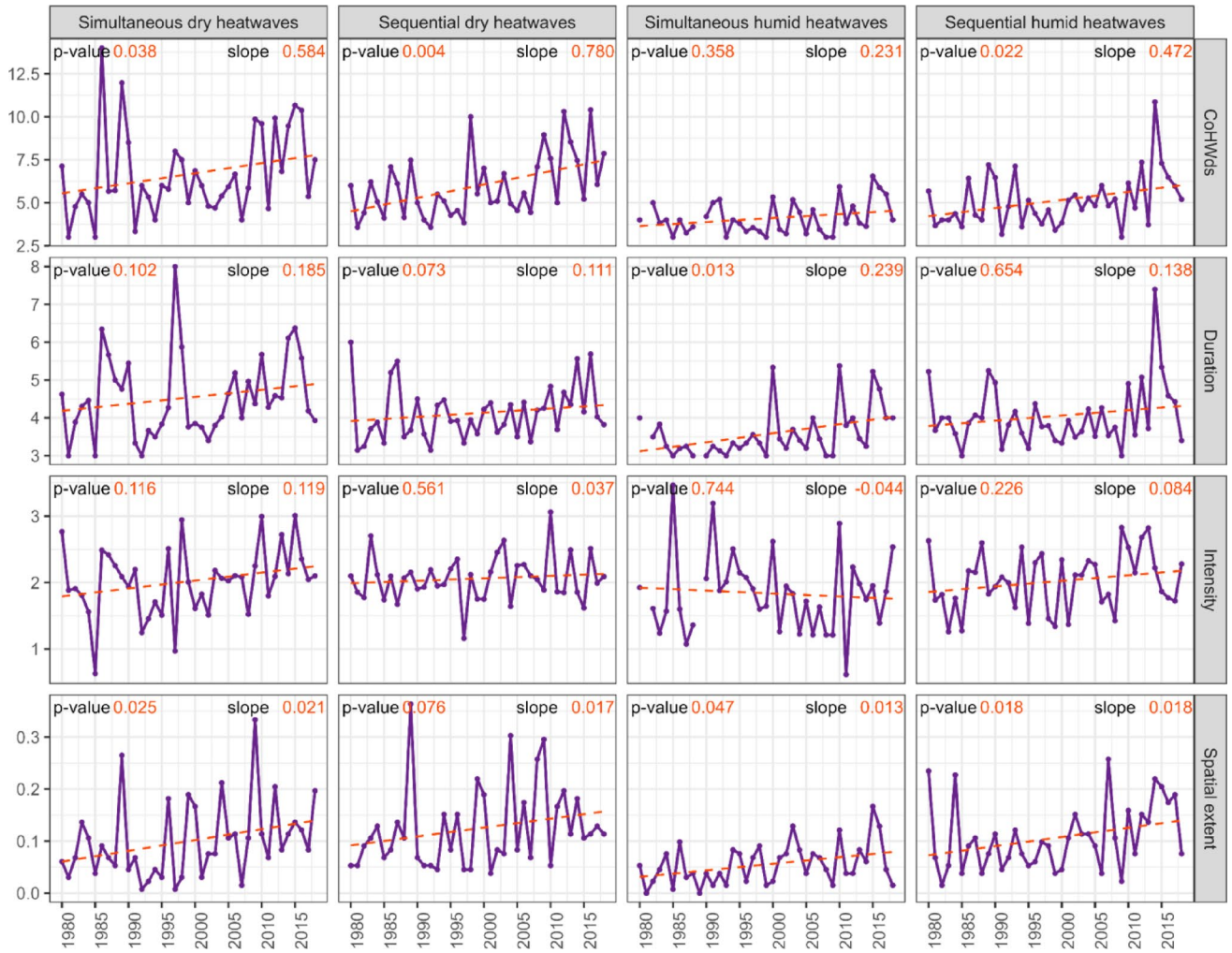

Fig. 5 Time series of CoHWds [days], duration [days], intensity [°C], and spatial extent [expressed as the percentage of stations with at least one event during the warm season] for SIDH, SEDH, SIHH, and SEHH. The *p*-values from the Mann–Kendall test for trend and the slope values (expressed as the rate of change for each variable every 10 years) are shown

Focusing on the duration, SIDH increased significantly in Regions 2 (CES) and 3 (CA), while SEDH showed a positive trend in Region 5 (SS). However, no significant changes were found for the duration of SIHH and SEHH across any regions. As for intensity, most regions did not show significant changes, with Region 5 (SSA) being the exception, where an increase in the intensity of SIDH was observed.

Finally, the spatial extent of compound heatwaves showed significant increases in a few regions. SIDH showed significant increases in Regions 3 (CA) and 5 (SS). Region 5 (SS) also exhibited significant increases for SEHH. In contrast, no significant changes were observed for SEDH and SIHH across any region.

3.5 Frequency of compound events under different climate driver phases

Subsequently, we analyzed the influence of large-scale climate drivers over compound heatwaves. Figure 7 presents the analysis of the influence of ENSO phases. La Niña was significantly associated with dry events (SIDH and SEDH), while El Niño showed association with humid events (SIHH and SEHH), although statistical significance is generally limited for the latter. For SIDH, events were more frequent during La Niña, particularly in central and northeastern Argentina, where relative frequencies exceed 70%, and several stations showed statistically significant results. In contrast, SIDH events during El Niño were less frequent.

Similarly, SEDH were more common under La Niña conditions, especially in northeastern Argentina and the Pampas region, with scattered stations with significant results. However, in northwestern Argentina, the occurrence of SEDH

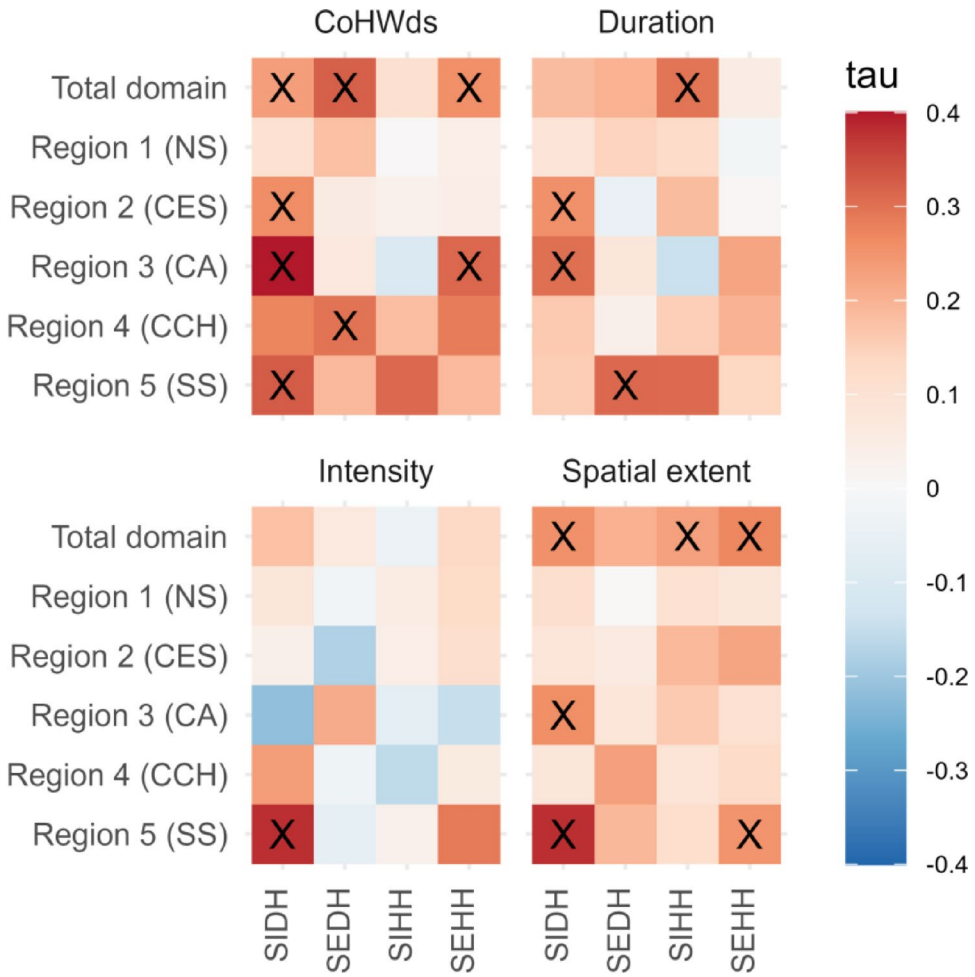

Fig. 6 Tau values from the Mann–Kendall test for the trend in total domain and regionally averaged (excluding Region 6, NCH) time series of CoHWds [days], duration [days], intensity [°C], and spatial extent (expressed as the proportion of stations per region that recorded events) for SIDH, SEDH, SIHH, and SEHH. Crosses indicate significant trends (5%)

seemed to be linked to El Niño. For SIHH and SEHH, a higher relative frequency of events was observed during El Niño, particularly in the northern and eastern parts of the study area. Despite these patterns, statistically significant associations were limited, which adds uncertainty to the strength of these relationships.

The results for the PDO are presented in Fig. 8. PDO− was associated with dry events (SIDH and SEDH), while PDO+ appeared to favor humid events (SIHH and SEHH). For SIDH, higher relative frequencies (>70%) were observed during PDO− across central and northeastern Argentina. In contrast, during PDO+, relative frequencies were lower (<30%). For SEDH, events were notably more frequent during PDO−, particularly in central Argentina, Uruguay and Chile. While PDO+ showed moderate relative frequencies overall, it is worth noting that some stations near northwestern Argentina exhibited more events during this phase. Humid events (SIHH and SEHH) did not exhibit a strong signal in response to PDO phases. However, certain stations near central Chile, parts of Brazil, and two stations in central and northeastern Argentina experienced higher frequencies of SEHH during PDO+.

Figures S4 and S5 in Online Resource 1 present the relative frequencies under the IOD and SAM phases, respectively. In both cases, the influence of these drivers on compound heatwave occurrence in SSA seemed to be weak. However, a few cases with significant associations were identified. For instance, SEDH events were more frequent under IOD− at a few stations in central and southern parts of the study area, while in some northern stations, they were more common under IOD+. Similarly, a limited number of stations in central Argentina and southern Chile showed higher relative frequencies of dry heatwaves (SIDH and SEDH) during SAM+. Despite these localized signals, no clear pattern of compound heatwave occurrence under the IOD and SAM phases was observed across SSA.

3.6 Influence of DCs on compound heatwave occurrence

Figure 9 shows the climatological occurrence of all possible combinations of drivers in bars. A more detailed breakdown of these combinations is provided in Table 2. This analysis provides a baseline for understanding their role in shaping

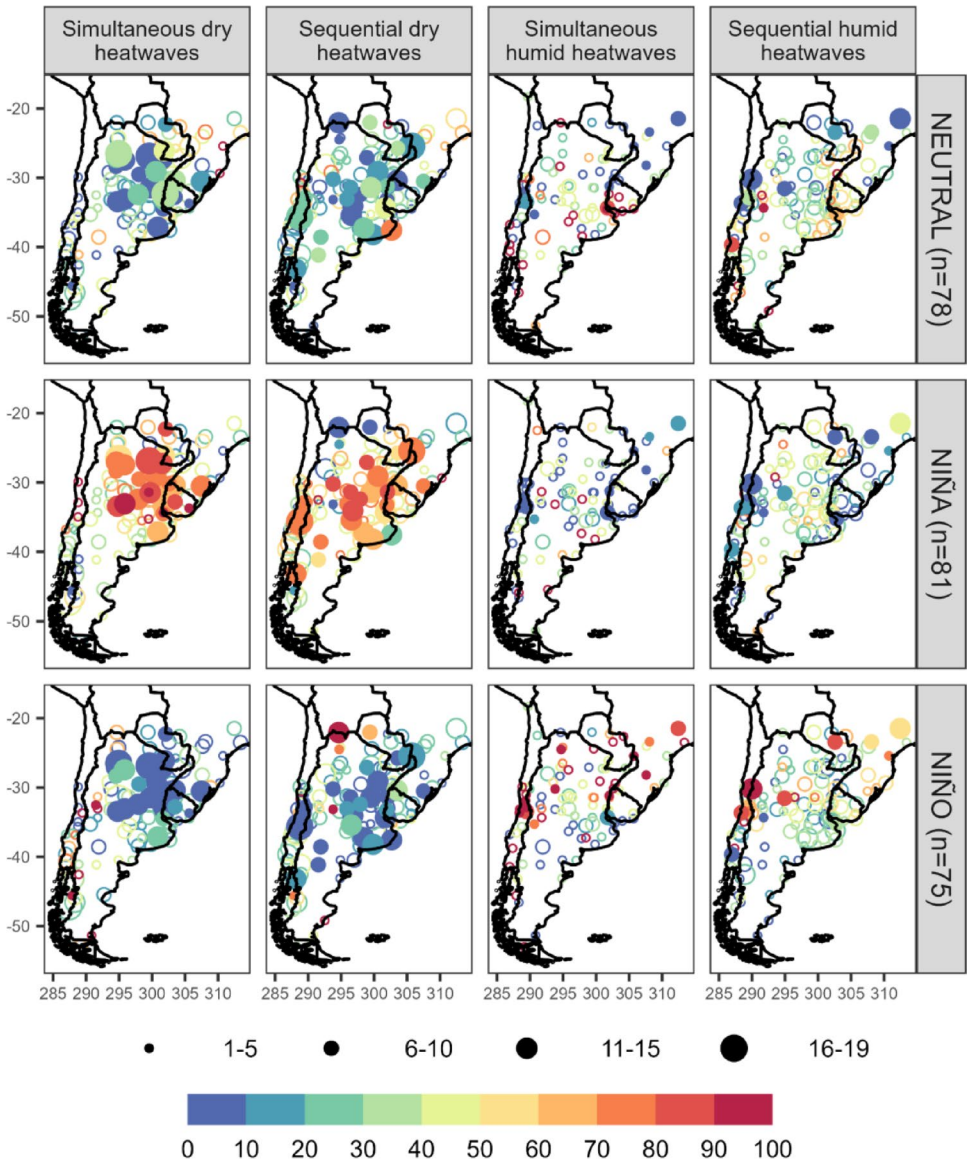

Fig. 7 Relative frequencies of events in each phase of ENSO (with respect to absolute frequency of event for each station). Point size indicates the absolute frequency of events (grouped into four categories). Filled circles represent results that are statistically significant at the 5% level according to Fisher's exact test. The "N" values near each driver phase indicate the total number of months in that phase during 1979–2018

compound heatwaves. The most frequent DC was DC 11 (Niña, PDO-, IOD-, SAM+), appearing in approximately 10% of the warm-season months during the study period. In contrast, DC 10 (Niño, PDO-, IOD-, SAM+) was the least frequent, observed in only 1 month. Other relatively frequent DCs included DC 1, DC 7, DC 9, and DC 13, each present in about 7–8% of the warm-season months (approximately 17 months).

In addition to this climatology, Fig. 9 also presents the time series of conditional probabilities for each type of compound heatwave (SIDH, SEDH, SIHH, and SEHH) across the five regions of SSA. By combining these probabilities and the climatology of all DCs, we can assess whether certain DCs tend to enhance or inhibit the occurrence of compound heatwaves, regardless of DC overall frequency.

Overall, DC 11 emerged as one of the most influential configurations. Defined by La Niña conditions, negative PDO and IOD phases, and a positive SAM, this DC tended to promote dry heatwaves. La Niña and IOD– combination also appeared in other DCs associated with SIDH and SEDH occurrences (DC 8, DC 20). Two additional DCs, DC 3 and DC 4, were notable for their association with a reduced occurrence of dry heatwaves. Both are characterized by El Niño or neutral ENSO phases and a positive IOD. However, they differ in the PDO phase: positive in DC 3 and negative in DC 4. While a positive SAM phase was present in many of the DCs that influence dry heatwaves, its role seems ambiguous, as it does not consistently align with either promoting or inhibiting these events.

As for humid heatwaves, DC 11 again stood out, this time for its suppressive effect across several regions of

Fig. 8 Same as Fig. 7, but for PDO

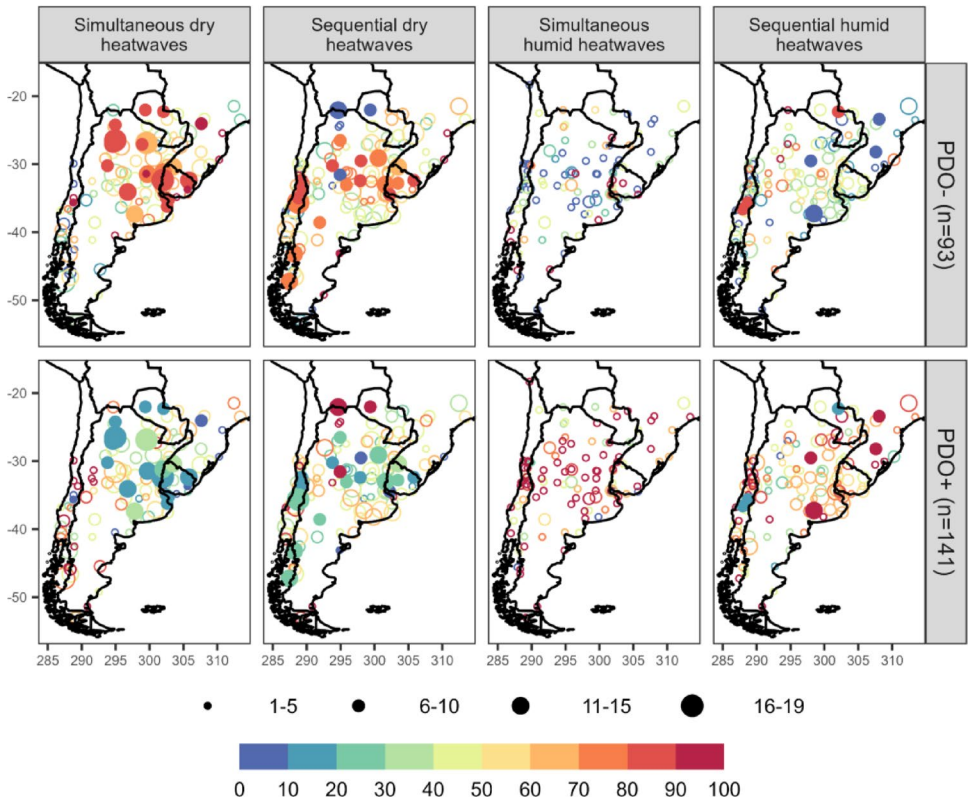

Fig. 9 Probability of occurrence of each DC (bars) and conditional probability of compound heatwave occurrence given each DC (lines), for each region (excluding Region 6, NC). Bars represent the climatology of DCs (calculated as the absolute frequency of each DC relative to the total number of warm-season months). Lines indicate the conditional probability of a compound heatwave occurring under each DC, which is represented as the proportion of compound heatwave months associated with each DC, relative to the total number of compound heatwave months across the entire period

Table 2 All 24 possible combinations of climate drivers phases (DC). Absolute frequency of each DC in 1979–2018 is also shown

Driver combination	ENSO	PDO	IOD	SAM	DC Frequency (months)
DC 1	NIÑO	PDO+	IOD+	SAM+	19
DC 2	NIÑA	PDO+	IOD+	SAM+	9
DC 3	NEUTRAL	PDO+	IOD+	SAM+	7
DC 4	NIÑO	PDO-	IOD+	SAM+	4
DC 5	NIÑA	PDO-	IOD+	SAM+	10
DC 6	NEUTRAL	PDO-	IOD+	SAM+	8
DC 7	NIÑO	PDO+	IOD-	SAM+	17
DC 8	NIÑA	PDO+	IOD-	SAM+	10
DC 9	NEUTRAL	PDO+	IOD-	SAM+	19
DC 10	NIÑO	PDO-	IOD-	SAM+	1
DC 11	NIÑA	PDO-	IOD-	SAM+	24
DC 12	NEUTRAL	PDO-	IOD-	SAM+	12
DC 13	NIÑO	PDO+	IOD+	SAM-	17
DC 14	NIÑA	PDO+	IOD+	SAM-	7
DC 15	NEUTRAL	PDO+	IOD+	SAM-	6
DC 16	NIÑO	PDO-	IOD+	SAM-	6
DC 17	NIÑA	PDO-	IOD+	SAM-	4
DC 18	NEUTRAL	PDO-	IOD+	SAM-	5
DC 19	NIÑO	PDO+	IOD-	SAM-	7
DC 20	NIÑA	PDO+	IOD-	SAM-	9
DC 21	NEUTRAL	PDO+	IOD-	SAM-	14
DC 22	NIÑO	PDO-	IOD-	SAM-	4
DC 23	NIÑA	PDO-	IOD-	SAM-	8
DC 24	NEUTRAL	PDO-	IOD-	SAM-	7

Fig. 10 Percentage of stations affected by each compound heatwave event under each DC, for each region (excluding Region 6, NC). Colors indicate the total number of events. Each point represents a certain number of events (given by the color), with the x-axis indicating the DC and the y-axis showing the percentage of stations affected within a region

SSA. Unlike dry events, humid heatwaves seemed to be more sensitive to the PDO phase, with positive PDO conditions enhancing their occurrence and negative PDO phases linked to their suppression. On the other hand, neither IOD nor SAM showed a consistent relationship with the occurrence of SIHH or SEHH events.

Other combinations also influence multiple event types. For instance, DC 20, which is characterized by the opposite configuration to DC 4 (La Niña, PDO+, IOD+, SAM–), was associated with an increased occurrence of simultaneous events (SIDH and SIHH) in several regions. Similarly, DC 7 (Neutral ENSO, PDO–, IOD+, SAM+) tended to promote SIDH, SEDH, and SEHH, particularly in southern regions.

We also considered the percentage of stations affected by each compound heatwave event under each DC (Fig. 10). This figure allows us to evaluate not only how DCs influence compound heatwave frequency, but also how widespread those events tend to be. In this context, dry heatwaves tended to affect a larger portion of meteorological stations under certain DCs, especially DC 5, DC 7 and DC 11. For instance, SIDH events under DC 5 in Region 2 (CES) and DC 7 in Region 5 (SS) reached over 50% of the stations. In contrast, humid heatwaves generally exhibited a more limited spatial extent. Most SIHH and SEHH events affected only a few stations, with some exceptions such as SEHH events under DC 9 in Region 5 (SS), where two events affected more than half of the stations. These findings also highlight that spatial extent does not always align with frequency. For example, DC 20 was linked to an increased occurrence of simultaneous events, especially dry ones, yet these remained spatially limited.

4 Discussion

The occurrence of compound events in SSA is strongly shaped by both land–atmosphere feedbacks and large-scale climate variability. For instance, dry conditions can intensify surface heating through reduced soil moisture and limited evaporative cooling, enhancing the likelihood of hot and dry extremes (Zscheischler and Seneviratne 2017; Guntu et al. 2023). By contrast, compound hot and humid events are more dependent on boundary-layer moisture availability and large-scale atmospheric moisture transport (Raymond et al. 2021), which can moderate temperature increases and may limit the frequency and persistence of humid compound extremes.

Our results reflect these underlying mechanisms. Dry heatwaves, both simultaneous (SIDH) and sequential (SEDH), were the most frequent types of compound events, especially in central and northeastern Argentina. Humid heatwaves showed a more heterogeneous spatial distribution, with SEHH occurring more often than SIHH, particularly in central-eastern Argentina, Uruguay, and parts of Chile.

These spatial patterns align with the well-known land–atmosphere coupling in SESA, especially over the La Plata Basin during the warm season (Sörensson et al. 2010; Menéndez et al. 2016; Spennemann et al. 2018). In this region, dry spells and soil moisture deficits are known to intensify heat events by reducing the land's capacity for evaporative cooling (Coronato et al. 2020), reinforcing the predominance of dry compound heatwaves.

Moreover, our spatial results are consistent with earlier studies that identified northeastern and eastern Argentina as hotspots for compound heat and drought conditions (Olmo et al. 2022). Ridder et al. (2020) reported some of the highest global frequencies of concurrent hot and dry extremes in these areas. Similarly, Lopez-Ramírez et al. (2024) found that simultaneous hot and dry months were most common in northeastern Argentina and the Pampas, while hot months preceded by dry conditions prevailed in northwestern Argentina and the central-eastern Pampas. These regional patterns closely match the spatial distribution of SIDH and SEDH identified in our analysis.

Global warming is increasing the likelihood of heatwaves worldwide, and when combined with changes in precipitation, they contribute to more frequent compound hot and dry events (Bevacqua et al. 2022; Geirinhas et al. 2021). Future projections show a clear increase in the annual frequency of compound hot/dry events in SSA, with more than two events per year expected compared to the 1979–2014 baseline (Collazo et al. 2023).

Our results already reveal significant shifts in the frequency and spatial extent of compound heatwaves in recent decades. When comparing the periods 1979–1998 and 1999–2018, dry events (SIDH and SEDH) and SEHH became more frequent across SSA. These observed changes are consistent with trends reported for SSA. For instance, Pierrestegui et al. (2024) showed an increase of short-term hydrometeorological hazards in northeastern Argentina, southern Brazil, and southeastern Paraguay, including more frequent heatwaves and flash droughts and heavy precipitation. The increment of SIDH and SEDH events can also be linked to increased frequency of compound dry-hot extremes under drier soil conditions (Spennemann et al. 2018; Coronato et al. 2020).

At regional scale, SIDH showed changes in several regions, especially in Central Argentina and southern SSA (Regions 3 and 5). Our results suggest that these compound events are becoming more frequent and affecting larger areas, although their duration and intensity have remained mostly unchanged. For humid events, changes were more limited and spatially heterogeneous, with SEHH showing some regional increases in spatial extent, mainly in southern SSA (Region 5).

While land–atmosphere feedbacks help explain many of the observed spatial and temporal patterns, large-scale climate variability also plays a critical role. La Niña and El Niño, the two main phases of the ENSO, have distinct impacts on temperature and precipitation extremes in SSA due to their influence on atmospheric circulation and moisture transport (Grimm et al. 2000; Cai et al. 2020; Reboita et al. 2021). We demonstrate that, during La Niña phases, dry heatwaves (SIDH and SEDH) were more frequent, particularly in central and northeastern Argentina, with some stations showing statistically significant results. Conversely, El Niño conditions were associated with a higher frequency of humid heatwaves (SIHH and SEHH), although the statistical significance was limited. La Niña typically leads to circulation patterns that suppress rainfall and promote heat, while El Niño can enhance moisture transport from the Atlantic Ocean and western Amazon basin to SESA region, moderating extreme heat and increasing humidity (Silva et al. 2010; Rusticucci et al. 2017; Collazo et al. 2023; Lopez-Ramirez et al. 2024).

In the case of PDO, negative phases (PDO−) favored dry events, especially in central Argentina and Uruguay, while positive phases (PDO+) were linked to more humid heatwaves in certain regions. According to Reboita et al. 2021, the cold phase of the PDO is characterized by negative precipitation anomalies over central-eastern South America, including central Argentina and Uruguay. This dryness can be linked to an increased likelihood of dry heatwaves in these regions under PDO−. Conversely, the warm PDO phase is associated with positive precipitation anomalies and wetter conditions in central-eastern South America, supporting the

prevalence of humid heatwaves during PDO+phases. This dipole in precipitation linked to PDO phases thus modulates the occurrence of dry versus humid heatwaves in this region.

Although the IOD showed weaker and more spatially limited effects on compound heatwaves in our analysis, previous studies have suggested potential teleconnections between the IOD and South American climate. In particular, positive IOD phases have been associated with a Rossby wave train extending from the southeastern Indian Ocean to the South Pacific and South Atlantic, potentially influencing surface air temperature and precipitation over SSA, including the La Plata Basin (Chan et al. 2008; Reboita et al. 2021). Some studies also suggest enhanced precipitation in this region during positive IOD events, partly due to an anomalous low-level anticyclone over the South Atlantic and increased moisture transport by the South American Low-Level Jet (Chan et al. 2008). However, these impacts appear to be strongest during the austral spring and can be often overshadowed by concurrent ENSO activity.

Similar to the IOD, the SAM showed weaker and more localized impacts on compound heatwaves in our analysis. Positive SAM phases (SAM+) appeared to enhance dry events in parts of Argentina and Chile, although no consistent regional pattern emerged. These findings align with previous studies that reported negative correlations between SAM and extreme precipitation indices in central Chile, suggesting that SAM+may contribute to drier conditions in this area (Iacobone et al. 2024). Given the importance of precipitation variability and extreme rainfall for economic sectors such as agriculture and hydroelectric power generation in the La Plata Basin (Peñalba and Robledo 2010; Iacobone et al. 2024), even localized SAM-related anomalies may have relevant socio-environmental implications.

When analyzing the combined phases of the drivers, certain configurations were found to have a significant influence. The combination of La Niña, PDO-, IOD-, and SAM+(DC 11) was associated in our study with a higher occurrence of dry heatwaves and a reduction in humid ones. This result aligns with previous studies showing that when ENSO and PDO are in the same phase, particularly both in cold phases, they can act constructively, reinforcing La Niña-related anomalies and intensifying drought conditions across South America (Kayano and Andreoli 2007; Reboita et al. 2021; Collazo et al. 2023). This may enhance subsidence and reduce moisture transport, favoring dry extremes.

On the other hand, IOD modulates ENSO teleconnections by merging the Indian Ocean wave train with the Pacific South American (PSA) pattern over the Pacific Ocean, especially for El Niño and positive IOD combination. La Niña and negative IOD exhibits strong inter-event variability and may not have a clear joint influence pattern. However, when both events are intense (strong La Niña and moderate or strong IOD-) their joint occurrence becomes more evident and produces an impact on the large-scale circulation, reinforcing subsidence and anticyclonic anomalies over SSA (Andrian et al. 2024). This circulation pattern inhibits precipitation and favors clear skies and high surface temperatures, helping to explain the increased occurrence of dry heatwaves and the reduction of humid ones under this configuration.

Regarding SAM, although its relationship with ENSO is complex and seasonally dependent, it has been observed that SAM+tends to occur during La Niña events and may enhance the PSA pattern under such conditions (Fogt et al. 2011; Reboita et al. 2021), potentially contributing to more persistent dry conditions. These findings highlight the importance of considering the combined phase of multiple drivers, as their interactions can amplify or reduce individual effects on compound heatwave occurrence.

Additionally, the combined phases of large-scale drivers could provide valuable information for statistical models of compound heatwaves. While our analysis focused on simultaneous associations rather than predictive relationships, and forecasts would also depend on reliable predictions of the drivers themselves, these findings contribute to a growing understanding that can support future efforts to model and anticipate compound heatwave occurrence.

5 Summary and conclusion

This study analyzes the spatial and temporal variability of compound heatwaves in SSA over the warm season from 1979 to 2018, using daily maximum temperature and precipitation records from 132 meteorological stations. By examining simultaneous and sequential heatwaves in combination with dry and humid conditions (SIDH, SEDH, SIHH, SEHH), we were able to capture how these compound events vary across SSA. Dry compound heatwaves were considerably more frequent than humid ones, particularly in central and northeastern SSA, consistent with known land–atmosphere feedback mechanisms in the region. In contrast, humid events were more spatially heterogeneous, with SEHH occurring more often than SIHH.

The heatwave regionalization allowed us to identify the diverse behaviors of compound heatwaves in specific areas, providing insights into how frequency, duration, intensity, and spatial extent of these events have evolved in recent decades. The comparison between the two sub-periods and the regional trends analysis revealed significant changes in frequency and spatial extent of several compound heatwaves, especially dry ones.

Additionally, we examined the role of large-scale climate drivers in modulating compound heatwaves. ENSO

and PDO emerged as the dominant modes of variability. In particular, La Niña conditions and negative PDO phases were linked to an increase in dry compound heatwaves, while El Niño and PDO + tended to favor humid events in some regions. In contrast, the influence of IOD and SAM was weaker and more spatially limited. Among all combinations, the configuration defined by La Niña, PDO −, IOD −, and SAM + (DC11) was identified as one of the most relevant, associated with a higher occurrence and greater spatial extent of dry heatwaves and a suppression of humid ones. This highlights the importance of considering both the individual and combined influence of large-scale drivers in understanding compound heatwaves in SSA.

Our results indicate which regions and climate patterns are most strongly linked to these events, providing valuable insights that can strengthen risk assessments and early warning systems. Moreover, the definitions and framework applied here can also be used to characterize compound heatwaves in global and regional climate models, as they rely on temperature-precipitation relationships that are comparable across observational and simulated datasets, although model resolution and biases should be carefully considered. Future work could integrate climate model projections to assess how these patterns may evolve under different climate scenarios, providing essential information for adaptation and resilience planning in the face of climate change.

Supplementary Information The online version contains supplementary material available at https://doi.org/10.1007/s00382-025-08016-9.

Author contribution All authors contributed to the study conception, analysis and design. Material preparation, data collection were performed by Agustina Lopez-Ramirez. The first draft of the manuscript was written by Agustina Lopez-Ramirez and all authors commented on previous versions of the manuscript. All authors read and approved the final manuscript.

Funding This work was supported by the projects PICT2019-2019-02933, CONICET PIP 0333 (2021–2023), UBACyT 20020220200111BA. S.C. acknowledges the SAFETE project, which has received funding from the European Union's Horizon 2020 research and innovation program under the Marie Skłodowska-Curie grant agreement No 847635 (UNA4CAREER).

Data availability The datasets generated in this study are available from the corresponding author upon reasonable request. Climate drivers datasets have public access online via the following links: ONI http://www.cpc.ncep.noaa.gov/, PDO https://psl.noaa.gov/data/climateindices/list/, IOD https://www.cpc.ncep.noaa.gov/products/international/ocean_monitoring/indian/IODMI/DMI_month.html and SAM http://www.nerc-bas.ac.uk/icd/gjma/sam.html.

Declarations

Conflict of interest The authors declare no conflict of interest.

References

Allen CD, Macalady AK, Chenchouni H, Bachelet D, McDowell N, Vennetier M, Cobb N (2010) A global overview of drought and heat-induced tree mortality reveals emerging climate change risks for forests. Forest Ecol Manage 259(4):660–684. https://doi.org/10.1016/j.foreco.2009.09.001

Andreoli RV, Kayano MT (2005) ENSO-related rainfall anomalies in South America and associated circulation features during warm and cold Pacific decadal oscillation regimes. Int J Climatol 25(15):2017–2030. https://doi.org/10.1002/joc.1222

Andrian LG, Osman M, Vera CS (2024) The role of the Indian Ocean Dipole in modulating the austral spring ENSO teleconnection to the Southern Hemisphere. Weather Clim Dynam 5(4):1505–1522. https://doi.org/10.5194/wcd-5-1505-2024

Ben-Ari T, Boé J, Ciais P, Lecerf R, Van der Velde M, Makowski D (2018) Causes and implications of the unforeseen 2016 extreme yield loss in the breadbasket of France. Nat Commun 9:1627. https://doi.org/10.1038/s41467-018-04087-x

Bevacqua E, Zappa G, Lehner F, Zscheischler J (2022) Precipitation trends determine future occurrences of compound hot–dry events. Nat Clim Chang 12:350–355. https://doi.org/10.1038/s41558-022-01309-5

Cai W, McPhaden MJ, Grimm AM, Rodrigues RR, Taschetto AS, Garreaud RD, Vera C et al (2020) Climate impacts of the El Niño-Southern Oscillation on South America. Nat Rev Earth Environ 1:215–231. https://doi.org/10.1038/s43017-020-0040-3

Carvalho LM, Jones C, Ambrizzi T (2005) Opposite phases of the Antarctic Oscillation and relationships with intraseasonal to interannual activity in the tropics during the austral summer. J Climate 18:702–718. https://doi.org/10.1175/JCLI-3284.1

Chan SC, Behera SK, Yamagata T (2008) Indian Ocean dipole influence on South American rainfall. Geophys Res Lett 35:L14706. https://doi.org/10.1029/2008GL034204

Collazo S, Barrucand M, Rusticucci M (2019) Summer seasonal predictability of warm days in Argentina: statistical model approach. Theor Appl Climatol 138:1853–1876. https://doi.org/10.1007/s00704-019-02933-6

Collazo S, Barrucand M, Rusticucci M (2023) Hot and dry compound events in South America: present climate and future projections, and their association with the Pacific Ocean. Nat Hazards 119:299–323. https://doi.org/10.1007/s11069-023-06119-2

Coronato T, Carril AF, Zaninelli PG, Giles J, Ruscica R, Falco M, Menéndez CG et al (2020) The impact of soil moisture–atmosphere coupling on daily maximum surface temperatures in Southeastern South America. Clim Dyn 55:2543–2556. https://doi.org/10.1007/s00382-020-05399-9

De Luca P, Donat MG (2023) Projected changes in hot, dry, and compound hot-dry extremes over global land regions. Geophys Res Lett 50:e2022GL102493. https://doi.org/10.1029/2022GL102493

Flannigan MD, Krawchuk MA, de Groot WJ, Wotton BM, Gowman LM (2009) Implications of changing climate for global wildland fire. Int J Wildland Fire 18:483–507. https://doi.org/10.1071/WF08187

Fogt RL, Bromwich DH, Hines KM (2011) Understanding the SAM influence on the South Pacific ENSO teleconnection. Clim Dyn 36:1555–1576. https://doi.org/10.1007/s00382-010-0905-0

Gamelin BL, Carvalho LM, Kayano MT (2020) The combined influence of ENSO and PDO on the spring UTLS ozone variability in South America. Clim Dyn 55:1539–1562. https://doi.org/10.1007/s00382-020-05340-0

Geirinhas JL, Russo A, Libonati R, Sousa PM, Miralles DG, Trigo RM (2021) Recent increasing frequency of compound summer drought and heatwaves in Southeast Brazil. Environ Res Lett 16:034036. https://doi.org/10.1088/1748-9326/abe0eb

Grimm AM, Barros VR, Doyle ME (2000) Climate variability in southern South America associated with El Niño and La Niña events. J Climate 13:35–58. https://doi.org/10.1175/1520-0442(2000)013%3c0035:CVISSA%3e2.0.CO;2

Guntu RK, Merz B, Agarwal A (2023) Increased likelihood of compound dry and hot extremes in India. Atmos Res 290:106789. https://doi.org/10.1016/j.atmosres.2023.106789

Guo Y, Huang Y, Fu Z (2023) What causes compound humidity-heat extremes to have different coupling strengths over the mid-lower reaches of the Yangtze River? Clim Dyn 60:4099–4109. https://doi.org/10.1007/s00382-022-06532-6

Hao Z, AghaKouchak A, Phillips TJ (2013) Changes in concurrent monthly precipitation and temperature extremes. Environ Res Lett 8:034014. https://doi.org/10.1088/1748-9326/8/3/034014

Hao Z, Hao F, Xia Y, Feng S, Sun C, Zhang X, Meng Y et al (2022) Compound droughts and hot extremes: characteristics, drivers, changes, and impacts. Earth-Sci Rev 235:104241. https://doi.org/10.1016/j.earscirev.2022.104241

Iacovone MF, Pántano VC, Penalba OC (2024) The relationship between ENSO, IOD and SAM with extreme rainfall over South America. Stoch Environ Res Risk Assess 38(5):1769–1782. https://doi.org/10.1007/s00477-023-02653-4

Ionita M, Caldarescu DE, Nagavciuc V (2021) Compound hot and dry events in Europe: variability and large-scale drivers. Front Clim 3:688991. https://doi.org/10.3389/fclim.2021.688991

Jiang Y, Huang B (2000) Effects of drought or heat stress alone and in combination on Kentucky bluegrass. Crop Sci 40(5):1358–1362. https://doi.org/10.2135/cropsci2000.4051358x

Kayano MT, Andreoli RV (2007) Relations of South American summer rainfall interannual variations with the Pacific Decadal Oscillation. Int J Climatol 27(4):531–540. https://doi.org/10.1002/joc.1417

Lopez-Ramirez A, Barrucand M, Collazo S (2024) Compound hot and dry events in Argentina and their connection to El Niño-Southern Oscillation. Int J Climatol 44(15):5641–5654. https://doi.org/10.1002/joc.8657

Marshall GJ (2003) Trends in the Southern Annular Mode from observations and reanalyses. J Climate 16(24):4134–4143. https://doi.org/10.1175/1520-0442(2003)016%3c4134:TITSAM%3e2.0.CO;2

McKee TB, Doesken NJ, Kleist J (1993) The relationship of drought frequency and duration to time scales. In: Proceedings of the 8th Conference on Applied Climatology 17(22):179–183

Menéndez CG, Zaninelli PG, Carril AF, Sánchez E (2016) Hydrological cycle, temperature, and land surface atmosphere interaction in the La Plata Basin during summer: response to climate change. Clim Res 68(2–3):231–241. https://doi.org/10.3354/cr01373

Mueller B, Seneviratne SI (2012) Hot days induced by precipitation deficits at the global scale. Proc Natl Acad Sci U S A 109(31):12398–12403. https://doi.org/10.1073/pnas.1204330109

Mukherjee S, Ashfaq M, Mishra AK (2020) Compound drought and heatwaves at a global scale: the role of natural climate variability-associated synoptic patterns and land-surface energy budget anomalies. J Geophys Res Atmos 125(11):e2019JD031943. https://doi.org/10.1029/2019JD031943

Olmo M, Bettolli ML, Rusticucci M (2020) Atmospheric circulation influence on temperature and precipitation individual and compound daily extreme events: spatial variability and trends over southern South America. Weather Clim Extremes 29:100267. https://doi.org/10.1016/j.wace.2020.100267

Olmo M, Weber T, Teichmann C, Bettolli ML (2022) Compound events in south America using the CORDEX-CORE ensemble: current climate conditions and future projections in a global warming scenario. J Geophys Res Atmos 127(21):e2022JD037708. https://doi.org/10.1029/2022JD037708

Penalba OC, Robledo FA (2010) Spatial and temporal variability of the frequency of extreme daily rainfall regime in the La Plata Basin during the 20th century. Clim Change 98(3):531–550. https://doi.org/10.1007/s10584-009-9744-6

Pierrestegui, M J, Lovino, M A, Müller, G V, Müller, O V (2024). Multihazard assessment of long- and short-term extreme hydrometeorological events in southeastern South America. EGU General Assembly 2024, Vienna, Austria, 14–19 Apr 2024, EGU24-9257. https://doi.org/10.5194/egusphere-egu24-9257

Raymond C, Matthews T, Horton RM (2020) The emergence of heat and humidity too severe for human tolerance. Sci Adv 6(19):eaaw1838. https://doi.org/10.1126/sciadv.aaw1838

Raymond C, Matthews T, Horton RM, Fischer EM, Fueglistaler S, Ivanovich C et al (2021) On the controlling factors for globally extreme humid heat. Geophys Res Lett 48(23):e2021GL096082. https://doi.org/10.1029/2021GL096082

Reboita MS, Ambrizzi T, Crespo NM, Dutra LMM, Ferreira GWDS, Rehbein A et al (2021) Impacts of teleconnection patterns on South America climate. Ann N Y Acad Sci 1504(1):116–153. https://doi.org/10.1111/nyas.14592

Ridder NN, Pitman AJ, Westra S, Ukkola A, Do HX, Bador M et al (2020) Global hotspots for the occurrence of compound events. Nat Commun 11(1):5956. https://doi.org/10.1038/s41467-020-19639-3

Rusticucci M, Barrucand M and Collazo S (2017) Temperature extremes in the Argentina central region and their monthly relationship with the mean circulation and ENSO phases. Int. J. Climatol. 37:3003–3017. https://doi.org/10.1002/joc.4895

Seneviratne SI, Corti T, Davin EL, Hirschi M, Jaeger EB, Lehner I et al (2010) Investigating soil moisture–climate interactions in a changing climate: a review. Earth-Sci Rev 99(3–4):125–161. https://doi.org/10.1016/j.earscirev.2010.02.004

Seneviratne SI, Nicholls N, Easterling D, Goodess CM, Kanae S, Kossin J et al (2012) Changes in climate extremes and their impacts on the natural physical environment. In: Field CB, Barros V, Stocker TF et al (eds) Managing the risks of extreme events and disasters to advance climate change adaptation. Cambridge University Press, pp 109–230

Silva GAM, Ambrizzi T (2010) Summertime moisture transport over Southeastern South America and extratropical cyclones behavior during inter-El Niño events. Theor Appl Climatol 101:303–310. https://doi.org/10.1007/s00704-009-0218-6

Smirnov NV (1939) Estimate of deviation between empirical distribution functions in two independent samples. Bulletin Moscow University 2(2):3–16

Sörensson AA, Menéndez CG, Samuelsson P, Willén U, Hansson U (2010) Soil-precipitation feedbacks during the South American

monsoon as simulated by a regional climate model. Clim Change 98(3):429–447. https://doi.org/10.1007/s10584-009-9740-x

Spennemann PC, Salvia M, Ruscica RC, Sörensson AA, Grings F, Karszenbaum H (2018) Land-atmosphere interaction patterns in southeastern South America using satellite products and climate models. Int J Appl Earth Obs Geoinf 64:96–103. https://doi.org/10.1016/j.jag.2017.08.016

Suli S, Barriopedro D, García-Herrera R, Rusticucci M (2023) Regionalisation of heat waves in southern South America. Weather Clim Extremes 40:100569. https://doi.org/10.1016/j.wace.2023.100569

Tencer B, Bettolli ML, Rusticucci M (2016) Compound temperature and precipitation extreme events in southern South America: associated atmospheric circulation, and simulations by a multi-RCM ensemble. Clim Res 68(2–3):183–199

Wang G, Cai W (2013) Climate-change impact on the 20th-century relationship between the Southern Annular Mode and global mean temperature. Sci Rep 3(1):2039. https://doi.org/10.1038/srep02039

Wang SSY, Kim H, Coumou D, Yoon JH, Zhao L, Gillies RR (2019) Consecutive extreme flooding and heat wave in Japan: are they becoming a norm? Atmos Sci Lett 20:e933. https://doi.org/10.1002/asl.933

Wu X, Jiang D (2022) Probabilistic impacts of compound dry and hot events on global gross primary production. Environ Res Lett 17(3):034049. https://doi.org/10.1088/1748-9326/ac4c5b

Zhang W, Luo M, Gao S, Chen W, Hari V, Khouakhi A (2021) Compound hydrometeorological extremes: drivers, mechanisms and methods. Front Earth Sci 9:673495. https://doi.org/10.3389/feart.2021.673495

Zscheischler J, Seneviratne SI (2017) Dependence of drivers affects risks associated with compound events. Sci Adv 3(6):e1700263. https://doi.org/10.1126/sciadv.1700263